Neutron scattering measurements of critical exponents in CsMnBr$_3$: A $Z_2 \times S_1$ antiferromagnet

T. E. Mason

Department of Physics, McMaster University, Hamilton, Ontario, Canada L8S 4M1

B. D. Gaulin[*]

Solid State Division, Oak Ridge National Laboratory, Oak Ridge, Tennessee 37831

M. F. Collins

Department of Physics, McMaster University, Hamilton, Ontario, Canada L8S 4M1

(Received 11 July 1988)

CsMnBr$_3$ is an XY-like antiferromagnet on a stacked, triangular lattice with nearest-neighbor interactions. It orders antiferromagnetically at $T_N = 8.3$ K. We have used neutron scattering measurements of the frequency-integrated critical scattering in the paramagnetic state and magnetic Bragg peak intensity in the ordered state to determine the critical exponents γ, ν, and β. Based on these measurements we conclude that $\gamma = 1.01 \pm 0.08$, $\nu = 0.54 \pm 0.03$, and $\beta = 0.21 \pm 0.02$. These values do not correspond to any standard universality class characterized by the dimensionality of the lattice and the order parameter. They do, however, agree with predictions by Kawamura for a universality class characterized by the symmetry of the order parameter, $Z_2 \times S_1$. This symmetry differs from that of the standard XY model (S_1) due to the presence of chiral degeneracy (Z_2), a consequence of lattice frustration.

I. INTRODUCTION

The presence of frustration in magnetic systems can result in diverse phenomena, for example spin-glass behavior or incommensurate magnetically ordered states. Systems with somewhat less frustration and a commensurate ordered state can still exhibit unusual behavior not found in nonfrustrated cases. An example of this is an antiferromagnet on a stacked, triangular lattice where the lattice frustration results in noncollinear spin ordering with the spins on three sublattices forming 120° angles with nearest neighbors on the other sublattices.

The XY antiferromagnet on a stacked triangular lattice has two equivalent ground states differing in the sense of the spin rotation from sublattice to sublattice. This "chiral" degeneracy is in addition to the continuous rotational degeneracy present in both frustrated and nonfrustrated models. The order parameter of this system has symmetry $V = Z_2 \times S_1$ which differs from that of the standard XY model ($V = S_1$) due to the chiral degeneracy ($V = Z_z$), a consequence of the lattice frustration. This has led to predictions that the $Z_2 \times S_1$ antiferromagnet belongs to a distinct universality class with critical exponents $\gamma = 1.1 \pm 0.1$, $\nu = 0.53 \pm 0.03$, and $\beta = 0.25 \pm 0.02$.[1,2] A similar situation arises for the Heisenberg antiferromagnet on a stacked, triangular lattice where predictions that it belongs to the SO(3) universality class[2,3] have been confirmed by neutron scattering measurements of critical exponents for VCl$_2$.[4] Holmium and dysprosium form a different lattice but are predicted to belong to the $Z_2 \times S_1$ universality class by virtue of their spiral structure.[2] This prediction has been verified by recent neutron scattering measurements.[5]

CsMnBr$_3$ has a hexagonal lattice structure, space group $P6_3/mmc$, with $a = 7.61$ Å and $c = 6.52$ Å at room temperature.[6] The Mn^{2+} ions form a simple hexagonal lattice with a Mn-Mn separation of 3.26 Å along the c axis and 7.61 Å in the ab plane. Because the superexchange path along c is shorter and less complicated the antiferromagnetic interaction between the spin-$\frac{5}{2}$ Mn^{2+} magnetic moments is 460 times stronger along c than in the ab plane.[7] As a result of this anisotropic interaction CsMnBr$_3$ exhibits quasi-one-dimensional behavior above about 15 K.[8] The spins are restricted to the ab plane below 20 K by an anisotropy that is primarily dipolar in origin.

CsMnBr$_3$ undergoes three-dimensional antiferromagnetic ordering at 8.3 K with the spins in the ab plane. The maximum ordered moment has been determined experimentally to be $(3.0 \pm 0.3)\mu_B$.[9] This reduction from the theoretical value of $5\mu_B$ is believed to arise from quantum fluctuations in the frustrated state. Because the magnetic ions form a simple hexagonal lattice and the spins are restricted to two dimensions the transition is expected to belong to the $Z_2 \times S_1$ universality class. We have used neutron scattering techniques to determine the critical exponents and ascertain whether the XY antiferromagnet on a stacked, triangular lattice constitutes a universality class distinct from the standard XY model. Parts of the present work have been reported elsewhere in the literature.[10,11]

II. EXPERIMENTS AND RESULTS

The measurements were carried out on the $L3$ triple-axis spectrometer of the NRU reactor at the Chalk River

Nuclear Laboratories. An incident neutron energy of 3.3 THz was obtained using a silicon monochromator which supresses second-order contamination. A pyrolytic graphite filter was placed in the incident beam to remove any remaining contamination. The horizontal collimation before and after the sample was 0.3°. The vertical collimation was 1.3°. For measurements of the critical scattering above T_N the spectrometer was operated in double axis mode to measure the energy-integrated intensity in the static approximation. Measurements of the magnetic Bragg peak intensity below T_N were performed with a pyrolytic graphite analyzer set for zero-energy transfer.

Due to the potential effect of the presence of impurities on the critical properties of materials, great care was taken in growing the single-crystal sample of $CsMnBr_3$. Stoichiometric amounts of high-purity CsBr and $MnBr_2$ were initially mixed together and preheated under vacuum which allowed for both the removal of any hydrogenous contamination and the occurrence of the solid-state reaction. This charge was then loaded into a Bridgeman crucible and mounted in a Trans-Temp Bridgeman furnace. A large single-crystal sample was then produced by standard Bridgeman techniques. The material within the center of this single-crystal sample was separated from that at the top, bottom, and sides of the sample and this starting material was again placed in the same furnace and regrown into a single crystal by standard Bridgeman techniques. The resulting crystal was irregular in shape with dimensions in cm of $2 \times 1 \times 0.6$.

It was placed in a helium cryostat and oriented with (ξ, ξ, ζ) in the scattering plane. The mosaic was rather poor; there were two main crystallites separated by about 0.95°. The temperature was stable to ± 0.02 K. It was measured using a germanium sensor mounted on the heater block.

A. Sublattice magnetization below T_N

The magnetic Bragg peak intensity is proportional to the square of the sublattice magnetization. Near the critical temperature it should vary as a power law in reduced temperature with exponent 2β where β is the critical exponent corresponding to the order parameter. In order
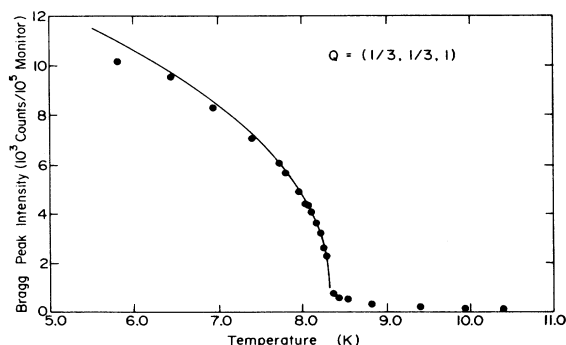
to determine β for $CsMnBr_3$ we have measured magnetic Bragg peak intensities as a function of temperature for $\mathbf{Q} = (\frac{1}{3}, \frac{1}{3}, 1)$, $(\frac{1}{3}, \frac{1}{3}, 3)$, and $(\frac{4}{3}, \frac{4}{3}, 1)$. Figure 1 shows the temperature dependence of the intensity at $(\frac{1}{3}, \frac{1}{3}, 1)$. The sharpness of the transition indicates that the sample temperature was at least as uniform as it was stable.

The three peaks measured had scattering angles of 25.0°, 70.5°, and 56.2°, respectively, and intensities in the ratio 11:2.5:1. Quite different extinction effects would be expected for the three peaks due to their different scattering geometries and intensities. Measurements made above T_N were used to determine the instrumental background and the correction due to critical scattering. The small critical scattering correction was made by fitting the data above T_N with a phenomenological third-degree polynomial in T which was reflected about T_N. This was then multiplied by an amplitude ratio and added to the temperature-independent instrumental background. The amplitude ratio used for the critical scattering below T_N was varied between 0 and 1 (there is less critical scattering below T_N). The fits for the critical exponent β described in Sec. III were not significantly affected by its value so an amplitude ratio of 0.5 was used for the critical scattering correction.

B. Critical scattering above T_N

The energy-integrated neutron intensity of the critical scattering above T_N was measured in scans along $(\xi, \xi, 1)$ from $\xi = 0$ to $\xi = 1$ and along $(\frac{1}{3}, \frac{1}{3}, \zeta)$ from $\zeta = 0.92$ to $\zeta = 1.08$ for temperatures between 8.45 and 11.90 K. Figure 2 illustrates the scans in reciprocal space, the inset shows the positions of the two crystallites relative to the two scans.

The resulting data were least-squares fitted to the standard Ornstein-Zernike expression for critical scattering
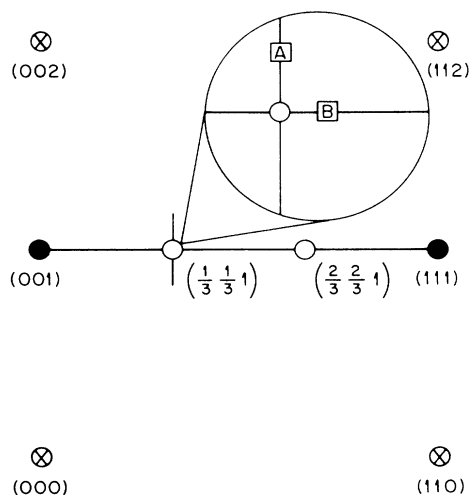

FIG. 1. Magnetic Bragg peak intensity as a function of temperature for $\mathbf{Q} = (\frac{1}{3}, \frac{1}{3}, 1)$. The line is the fit described in Sec. III with $\beta = 0.21$.

FIG. 2. Scans in reciprocal space for critical scattering above T_N. The inset shows the positions of the two main crystallines (denoted A and B) relative to the scans.
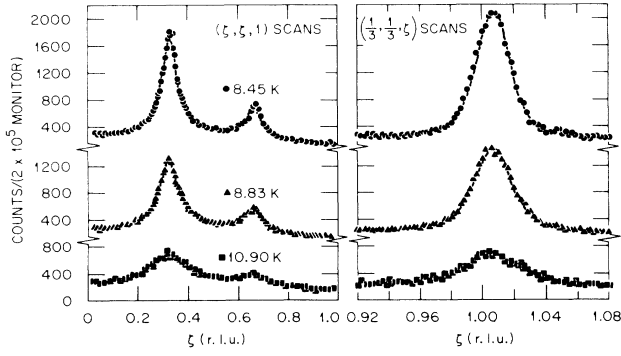
FIG. 3. Measured critical scattering along $(\xi,\xi,1)$ and $(\frac{1}{3},\frac{1}{3},\zeta)$ (in reciprocal lattice units) for $T=8.45$ K, $T=8.83$ K, and $T=10.90$ K. The lines are the fits to a Lorentzian convoluted with the spectrometer resolution with a linear background.

associated with three-dimensional ordering

$$I(Q) \propto \frac{\chi}{\left[1+\left[\dfrac{q}{\kappa_1}\right]^2\right]} f^2(Q) \ . \tag{1}$$

A linear background was assumed and the measurements were convoluted with the spectrometer resolution. χ is the sublattice susceptibility and κ_1 is the inverse correlation length. q is defined by $Q=q+\tau$ where τ is an antiferromagnetic reciprocal lattice vector. $f(Q)$ is the Mn^{2+} form factor. The horizontal resolution function was measured at 4.2 K. The vertical resolution was determined from the spectrometer configuration. Initially it was approximated as a triangle since this allows analytic integration out of the scattering plane. The sample was aligned with one of the two crystallites slightly above the scattering plane and the other slightly below. This was accounted for by introducing the estimated offset into the three-dimensional resolution function. Figure 3 shows the measured neutron intensity and the results of the fits for three temperatures.

In order to determine the importance of the vertical offset fits were also performed with no offset; one set with the actual spectrometer vertical resolution and another with a broader effective vertical resolution to approximate the effect of shifting the crystallites slightly out of the scattering plane. The significance of this with respect to the critical exponents is discussed further in Sec. III. The validity of approximating the Gaussian vertical resolution with a triangle was verified by fitting the data around $(\frac{1}{3},\frac{1}{3},1)$, with the background and critical scattering from $(\frac{2}{3},\frac{2}{3},1)$ subtracted (as determined from the previous fits), using a Gaussian vertical resolution. The results were not significantly affected indicating the triangular approximation was reasonable. Fits were done with backgrounds and peak positions fixed; they were also allowed to vary with temperature. The fitted values of χ and κ_1 were the same in both cases for all temperatures.
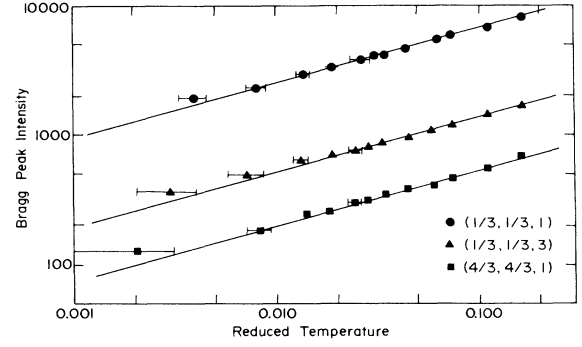
The data at the lowest temperature ($T=8.45$ K) were

FIG. 4. log-log plot of magnetic Bragg peak intensity (in relative units) as a function of reduced temperature for $Q=(\frac{1}{3},\frac{1}{3},1)$, $(\frac{1}{3},\frac{1}{3},3)$, and $(\frac{4}{3},\frac{4}{3},1)$. The lines are the results of a fit to a power law in reduced temperature with exponent $\beta=0.21$.

also least-squares fitted to the form suggested by Fisher and Burford[12] which includes the critical exponent η:

$$I(Q) \propto \frac{\chi}{\left[1+\left[1-\dfrac{\eta}{2}\right]^{-1}\left[\dfrac{q}{\kappa_1}\right]^2\right]^{(1-\eta/2)}} f^2(Q) \ . \tag{2}$$

Fits done with nonzero values of η were not better than those obtained using (1), the temperature was too far from T_N to observe deviations from the Lorentzian form.

III. CRITICAL EXPONENTS

The values for magnetic Bragg peak intensity (M_s^2), sublattice susceptibility (χ), and inverse correlation length (κ_1) were least-squares fitted to power laws in reduced temperature:

$$M_s^2 \propto \left[\frac{-(T-T_N)}{T_N}\right]^{2\beta} , \tag{3a}$$

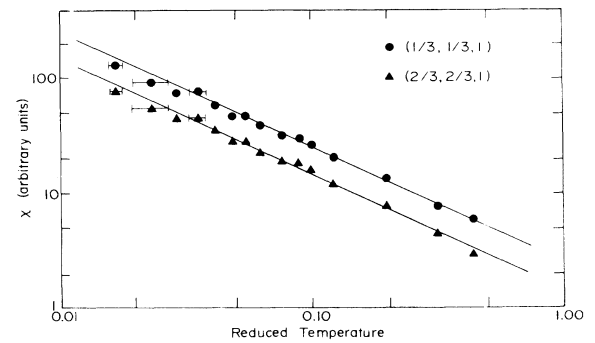$$\chi \propto \alpha \left[\frac{(T-T_N)}{T_N}\right]^{-\gamma} , \tag{3b}$$

FIG. 5. log-log plot of sublattice susceptibility (χ) as a function of reduced temperature for $Q=(\frac{1}{3},\frac{1}{3},1)$ and $(\frac{2}{3},\frac{2}{3},1)$. The lines are the results of a fit to a power law in reduced temperature with exponent $\gamma=1.01$.

$$\kappa_1 \propto \alpha \left[\frac{(T - T_N)}{T_N} \right]^v . \qquad (3c)$$

log-log plots for the three magnetic Bragg peak intensities, two sublattice susceptibilities [$(\frac{1}{3}, \frac{1}{3}, 1)$ and $(\frac{2}{3}, \frac{2}{3}, 1)$] and two inverse correlation lengths (along c and in the ab plane) are shown in Figs. 4, 5, and 6, respectively. The lines are the results of a fit to all the data with a single T_N; exponents for the same plots were constrained to be the same. There was a small variation of the fitted exponents with the critical temperature, T_N. This is shown in Fig. 7 where v and β have been scaled as indicated. Using T_N as a variable parameter resulted in a least-squares fit with $T_N = 8.31$ K, $\gamma = 1.01$, $v = 0.54$, and $\beta = 0.21$. The value of T_N is consistent with that previously obtained from the magnetic Bragg peak intensity data alone.[10]

Fits were also performed in which the data sets for each exponent were fitted with separate exponents [i.e., 3 β's for three different Bragg peaks, 2 γ's from $(\frac{1}{3}, \frac{1}{3}, 1)$ and $(\frac{2}{3}, \frac{2}{3}, 1)$, and $2v$'s for the c axis and the ab plane]. The resulting exponents differed only slightly from the values given above and the averages were the same. In the case of the magnetic Bragg peak intensity data this confirms that extinction was not a significant effect since any manifestation of extinction would be quite different for each peak. This is consistent with the fact that the ratio of the three intensities did not exhibit any temperature dependence.

In order to determine the significance of the approximations for the vertical resolution as discussed in Sec. II B fits were done using the values of χ and κ_1 obtained from the resolution convolutions with zero vertical offset. In both cases the largest effect was on the exponent γ which varies between 0.95 and 1.05 depending on the vertical resolution assumed. There was a similar effect on v but it was much smaller. Based on this and the estimated uncertainty in the least-squares fits to power-law behavior we conclude that $\gamma = 1.01 \pm 0.08$, $v = 0.54 \pm 0.03$, and $\beta = 0.21 \pm 0.02$ for CsMnBr$_3$. Subsequent to both this

FIG. 7. Variation of the fitted critical exponents with the critical temperature, T_N (K). v and β have been multiplied by 2 and 4, respectively, for clarity.

experiment and our analysis of the experimental data, we learned of an independent neutron scattering study of CsMnBr$_3$ performed just after our study. The critical exponents extracted from this work[13] are in agreement with our results presented here.

IV. CONCLUSIONS

The measured critical exponents for CsMnBr$_3$ are shown in Table I along with the theoretical predictions for the XY model[14] and the $Z_2 \times S_1$ universality class.[2] The experimental values do not agree with the predictions for the XY model or with the predictions for any standard model in which the universality class is characterized by the dimensionality of the lattice and the order parameter. They are, however, in good agreement with the predicted exponents for the $Z_2 \times S_1$ universality class, thus confirming that the XY antiferromagnet on a stacked, triangular lattice belongs to a universality class distinct from the standard XY model.

There is a hyperscaling relation relating γ, v, and β:

$$\gamma + 2\beta = dv , \qquad (4)$$

where d ($=3$) is the dimensionality of the system. If the covariance of the measured critical exponents with T_N (see Fig. 7) is neglected they are 1.5 standard errors away from satisfying (4). Exponents fitted with a slightly higher value of T_N are closer to satisfying (4) although for exact agreement the critical temperature ($T_N = 8.50$ K) is clearly too high. While it is not possible to draw definite conclusions as to the validity of hyperscaling for CsMnBr$_3$ it is interesting to note that the exponents mea-
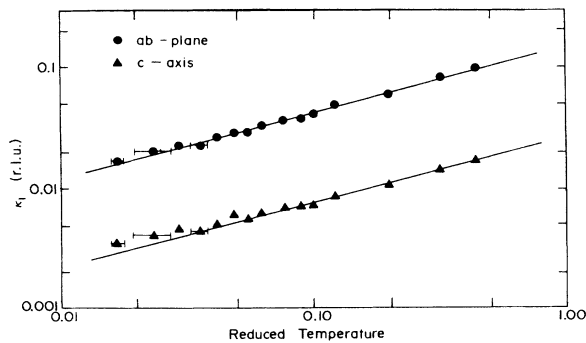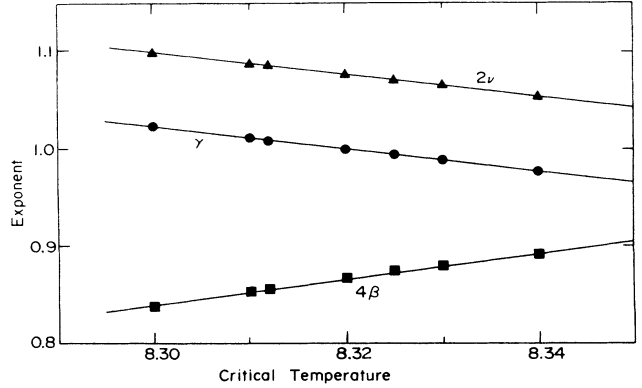

FIG. 6. log-log plot of inverse correlation length (κ_1) as a function of reduced temperature along the c axis and in the ab plane. The lines are the results of a fit to a power law in reduced temperature with exponent $v = 0.54$.

TABLE I. Measured critical exponents for CsMnBr$_3$ along with the theoretical predictions for the $Z_2 \times S_1$ universality class (Ref. 2) and the XY model (Ref. 14).

Exponent	Experimental	$Z_2 \times S_1$	XY model
γ	1.01 ± 0.08	1.1 ± 0.1	1.316 ± 0.009
v	0.54 ± 0.03	0.53 ± 0.03	0.669 ± 0.007
β	0.21 ± 0.02	0.25 ± 0.02	0.345 ± 0.011

sured for VCl_2 [SO(3) universality class] also fail to satisfy Eq. (4) by 2.6 standard errors in the same direction $(\gamma + 2\beta < 3\nu)$.[4]

ACKNOWLEDGMENTS

*Present address: Department of Physics, McMaster University, Hamilton, Ontario, Canada L8S 4M1.

[1] H. Kawamura, J. Phys. Soc. Jpn. **55**, 2095 (1986).

[2] H. Kawamura, J. Appl. Phys. **63**, 3086 (1988).

[3] H. Kawamura, J. Phys. Soc. Jpn. **54**, 3220 (1985).

[4] H. Kadowaki, K. Ubukoshi, K. Hirakawa, J. Martinez, and G. Shirane, J. Phys. Soc. Jpn. **56**, 4027 (1987).

[5] B. D. Gaulin, M. Hagen, and H. R. Child, J. Phys. (Paris) (to be published).

[6] J. Goodyear and D. J. Kennedy, Acta Crystallogr. **B28**, 1640 (1974).

[7] B. D. Gaulin, M. F. Collins, and W. J. L. Buyers, J. Appl. Phys. **61**, 3409 (1987).

[8] B. D. Gaulin and M. F. Collins, Can. J. Phys. **62**, 1132 (1984).

[9] M. Eibshutz, R. C. Sherwood, F. S. L. Hsu, and D. E. Cox, in *Magnetism and Magnetic Materials (Denver, 1972)*, Proceedings of the 18th Annual Conference on Magnetism and Magnetic Materials, AIP Conf. Proc. No. 10, edited by C. D. Graham, Jr. and J. J. Rhyne (AIP, New York, 1973), p. 684.

[10] T. E. Mason, M. F. Collins, and B. D. Gaulin, J. Phys. C **20**, L945 (1987).

[11] B. D. Gaulin, M. F. Collins, and and T. E. Mason, Physica B (to be published).

[12] M. E. Fisher and R. J. Burford, Phys. Rev. **156**, 583 (1967).

[13] H. Kadowaki, S. M. Shapiro, T. Inami, and Y. Ajiro, J. Phys. Soc. Jpn. **57**, 2640 (1988); Y. Ajiro, T. Nakashima, Y. Unno, H. Kadowaki, M. Mekata, and N. Achiwa, *ibid*. **57**, 2648 (1988).

[14] G. A. Baker, Jr., B. G. Nickel, and D. I. Meiron, Phys. Rev. B **17**, 1365 (1978).